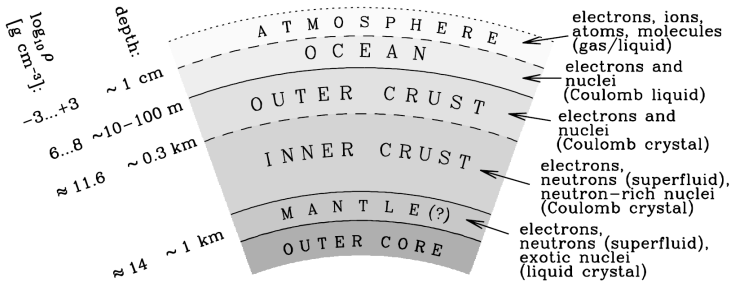


Unified equations of state for neutron stars

Nicolas Chamel
Institute of Astronomy and Astrophysics
Université Libre de Bruxelles, Belgium



Challenge



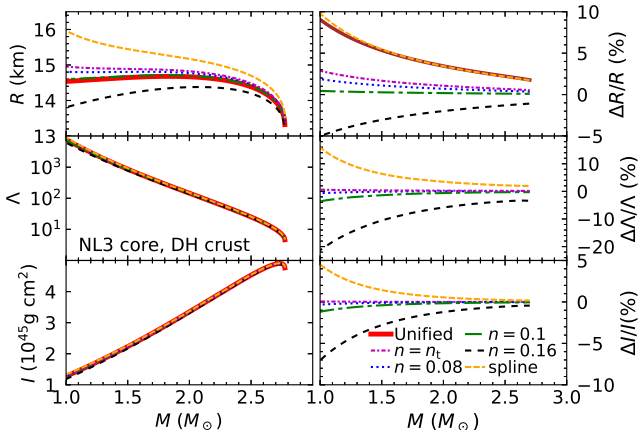
picture taken from Haensel, Potekhin, Yakovlev, "Neutron Stars" (Springer, 2007)

The interpretation of neutron-star observations requires not only the knowledge of the equation of state of dense matter but also the composition, the superfluid/superconducting properties, etc.

Blaschke&Chamel, Astrophys. Space Sci. Lib. 457, eds L. Rezzolla, P. Pizzochero, D. I. Jones, N. Rea, I. Vidaña p. 337-400 (Springer, 2018), arXiv:1803.01836

On the importance of a consistent description

Ad hoc matching of different models of dense matter can lead to
significant errors on the neutron-star structure & dynamics:



Outline

- ➊ Internal constitution of a neutron star
 - ▷ Microscopic model of dense matter
 - ▷ Constraints from laboratory experiments and ab initio calculations
- ➋ Comparison with astrophysical observations
 - ▷ Direct Urca cooling vs observed thermal emission
 - ▷ NICER view of PSR J0740+6620, PSR J0030+0451, PSR J0437–4715
 - ▷ Multimessenger observations of GW170817
- ➌ Conclusions & perspectives

Description of the outer crust of a neutron star

Traditional approach: numerical minimization of the Gibbs free energy per nucleon at different pressures P (cold catalyzed matter)

Tondeur, A&A 14, 451 (1971); Baym, Pethick, Sutherland, ApJ 170, 299 (1971)

- layers can be easily missed if δP not small enough!
- numerically costly (BPS considered 130 even nuclei vs $\sim 10^4$)

New approach: iterative minimization of the pressures between adjacent crustal layers (approximate analytical formulas)

Chamel, Phys. Rev. C 101, 032801(R) (2020)

- very accurate and reliable ($\delta P/P \sim 10^{-3}$ %)
- composition and stratification (depths, abundances)
- $\sim 10^6$ times faster

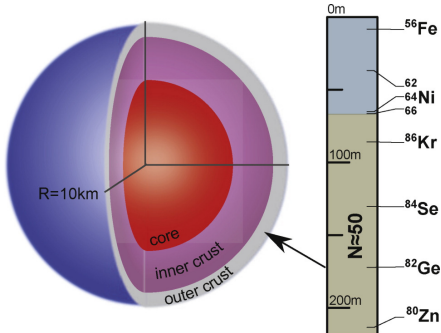
Freely available computer code:

<http://doi.org/10.5281/zenodo.3719439>

Nuclear-physics inputs: Masses of atomic nuclei

Experimentally determined layers

- The pressure is mainly given by the electron gas.
- The composition is completely determined by experimental data down to $\sim 200\text{m}$ for a $1.4M_{\odot}$ neutron star with $R = 10\text{ km}$.



Importance of magic nuclei

But constraints on Z due to beta equilibrium and electric charge neutrality

Few layers with $Z = 28$

Lack of measurements of neutron-rich nuclei with $Z \sim 40$ and $N \sim 82$

Kreim et al., Int.J.M.Spec.349-350,63(2013)

Wolf et al., Phys.Rev.Lett. 110,041101(2013)

Deeper, matter is treated via the **energy density functional theory**.

Nuclear energy-density functional theory

Many-body problem reduced to an effective one-body problem. This goes beyond the mean-field approximation.

In practice, one must solve the coupled **Hartree-Fock-Bogoliubov (HFB)** equations for both neutrons and protons ($q = n, p$):

$$\sum_{\sigma'} \begin{pmatrix} h'_q(\mathbf{r})_{\sigma\sigma'} & \Delta_q(\mathbf{r})\delta_{\sigma\sigma'} \\ \Delta_q(\mathbf{r})^*\delta_{\sigma\sigma'} & -\sigma\sigma' h'_q(\mathbf{r})_{-\sigma-\sigma'}^* \end{pmatrix} \begin{pmatrix} \psi_1^{(q)}(\mathbf{r}, \sigma') \\ \psi_2^{(q)}(\mathbf{r}, \sigma') \end{pmatrix} = \mathfrak{E}^{(q)} \begin{pmatrix} \psi_1^{(q)}(\mathbf{r}, \sigma) \\ \psi_2^{(q)}(\mathbf{r}, \sigma) \end{pmatrix}$$

$$h'_q(\mathbf{r})_{\sigma'\sigma} \equiv \left[-\nabla \cdot \frac{\delta E}{\delta \tau_q(\mathbf{r})} \nabla + \frac{\delta E}{\delta n_q(\mathbf{r})} - \lambda_q \right] \delta_{\sigma\sigma'} - i \frac{\delta E}{\delta \mathbf{J}_q(\mathbf{r})} \cdot \hat{\mathbf{\sigma}}_{\sigma'\sigma} + \dots$$

$n_q(\mathbf{r})$, $\tau_q(\mathbf{r})$, $\mathbf{J}_q(\mathbf{r})$, $\Delta_q(\mathbf{r})$... are defined from the density matrices

$$n_q(\mathbf{r}, \sigma; \mathbf{r}', \sigma') = \langle \Psi | c_q(\mathbf{r}', \sigma')^\dagger c_q(\mathbf{r}, \sigma) | \Psi \rangle$$

$$\tilde{n}_q(\mathbf{r}, \sigma; \mathbf{r}', \sigma') = -\sigma' \langle \Psi | c_q(\mathbf{r}', -\sigma') c_q(\mathbf{r}, \sigma) | \Psi \rangle,$$

which in turn depend on $\psi_1^{(q)}(\mathbf{r}, \sigma)$ and $\psi_2^{(q)}(\mathbf{r}, \sigma)$.

Description of the inner crust of a neutron star

Full 3D HFB calculations are computationally very costly in the inner crust and pasta mantle due to the presence of free neutrons.

Instead, we use the **Extended Thomas-Fermi (ETF)+Strutinsky Integral (SI)** method:

- **semiclassical expansion up to \hbar^4 :** the energy E becomes a functional of $n_q(\mathbf{r})$ and their derivatives only.
- **shell effects and pairing** are added consistently.
- different shapes are allowed: spheres, cylinders, slabs.
- to speed-up the computations, $n_q(\mathbf{r})$ are parametrized.

Pearson&Chamel, *Phys.Rev.C*105,015803(2022); *Phys.Rev.C*101,015802(2020)

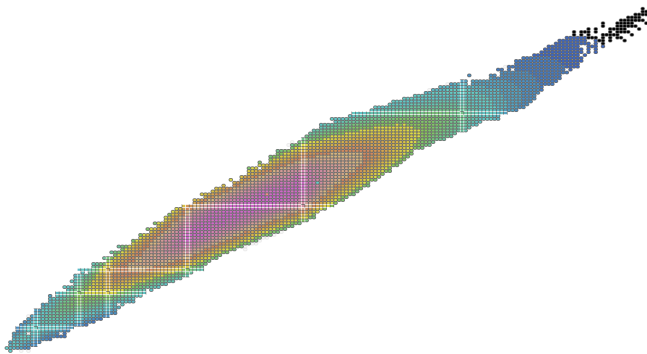
Pearson et al., *MNRAS* 481, 2994 (2018)

The ETFSI method is a **fairly accurate and computationally very fast** approximation to the full HFB equations

Shelley&Pastore, *Universe* 6, 206 (2020)

Brussels Skyrme functionals

They are based on **extended Skyrme and pairing interactions.**



<https://www-nds.iaea.org>

All are accurately calibrated to various experimental data:

- ~ 2300 atomic masses from AME (rms $\sim 0.5 - 0.6$ MeV/c 2)
- ~ 900 nuclear charge radii (rms ~ 0.03 fm)

Climbing the Jacob's ladder

- ▷ removal of spurious spin-isospin instabilities (BSk18)

$$v_{ij} \rightarrow v_{ij} + \frac{1}{2} t_4 (1 + x_4 P_\sigma) \frac{1}{\hbar^2} \left\{ p_{ij}^2 n(\mathbf{r})^\beta \delta(\mathbf{r}_{ij}) + \delta(\mathbf{r}_{ij}) n(\mathbf{r})^\beta p_{ij}^2 \right\}$$
$$+ t_5 (1 + x_5 P_\sigma) \frac{1}{\hbar^2} \mathbf{p}_{ij} \cdot n(\mathbf{r})^\gamma \delta(\mathbf{r}_{ij}) \mathbf{p}_{ij}$$

Chamel, Goriely, Pearson, Phys. Rev. C 80, 065804 (2009)

Chamel & Goriely, Phys. Rev. C 82, 045804 (2010)

- ▷ fit to realistic neutron-matter equations of state (BSk19-21)

Goriely, Chamel, Pearson, Phys. Rev. C 82, 035804 (2010)

- ▷ fit to different symmetry energies (BSk22-26)

Goriely, Chamel, Pearson, Phys. Rev. C 88, 024308 (2013)

- ▷ generalized spin-orbit coupling (BSk29)

$$\mathcal{E}_{\text{so}} = \frac{1}{2} \left[\mathbf{J} \cdot \nabla n + (1 + y_w) \sum_q \mathbf{J}_q \cdot \nabla n_q \right]$$

Goriely, Nucl. Phys. A 933, 68 (2015)

- ▷ fit to realistic 1S_0 pairing gaps (BSk30-32)

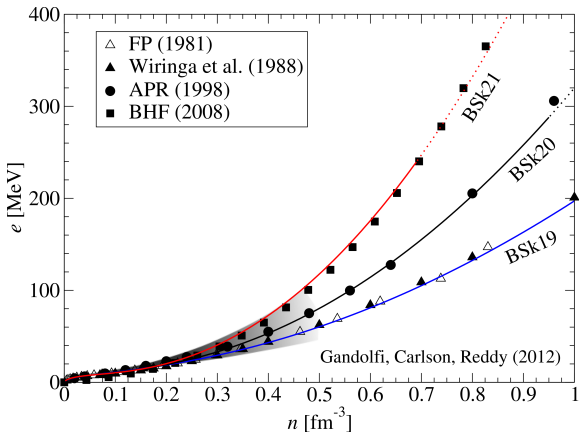
Goriely, Chamel, Pearson, Phys. Rev. C 93, 034337 (2016)

- ▷ new family using a full 3D HFB code (BSkG1-3)

Grams et al., EPJ A 59, 270 (2023)

BSk19-21: neutron-matter constraint

BSk19-21 were simultaneously fitted to three realistic neutron-matter equations of state with different degrees of stiffness:



BSk22-26: symmetry-energy constraints

BSk22-26 were further adjusted to different values of $J = S(n_0)$.

	BSk22	BSk23	BSk24	BSk25	BSk26
a_v [MeV]	-16.088	-16.068	-16.048	-16.032	-16.064
n_0 [fm^{-3}]	0.1578	0.1578	0.1578	0.1587	0.1589
J [MeV]	32.0	31.0	30.0	29.0	30.0
L [MeV]	68.5	57.8	46.4	36.9	37.5
K_{sym} [MeV]	13.0	-11.3	-37.6	-28.5	-135.6
K_v [MeV]	245.9	245.7	245.5	236.0	240.8
K' [MeV]	275.5	275.0	274.5	316.5	282.9
M_s^*/M	0.80	0.80	0.80	0.80	0.80
M_v^*/M	0.71	0.71	0.71	0.74	0.65
NeuM	BHF	BHF	BHF	BHF	APR

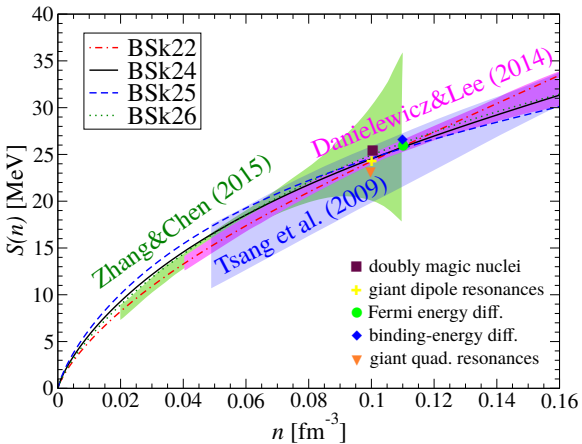
Lower and higher values of J were considered but yielded substantially worse fits to atomic masses.

BHF: 'V18' from *Li & Schulze, PRC 78, 028801 (2008)*

APR: 'A18 + δv + UIX*' from *Akmal et al., PRC 58, 1804 (1998)*

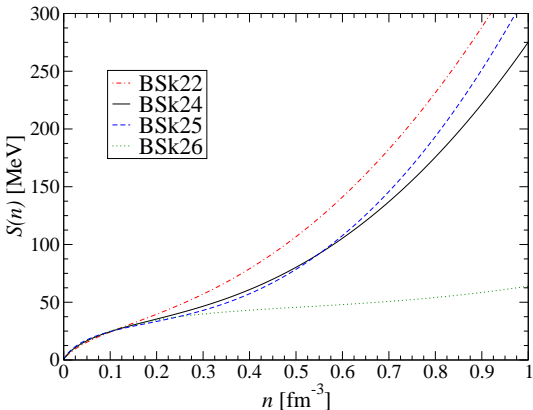
BSk22-26: symmetry-energy constraints

The symmetry energy $S(n)$ at lower densities is consistent with various experimental constraints:



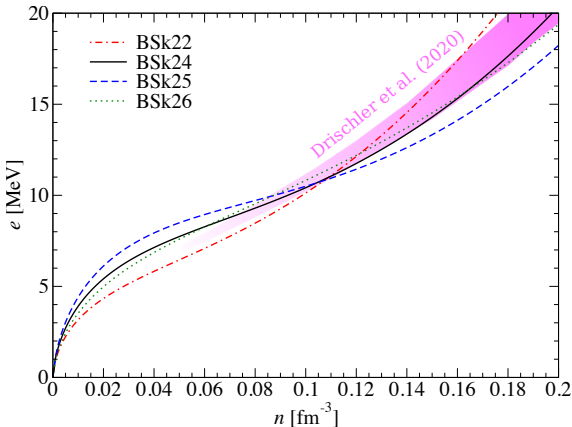
Symmetry energy at higher densities

BSk22-26 mainly differ in their predictions for the symmetry energy at densities encountered in the core of neutron stars:



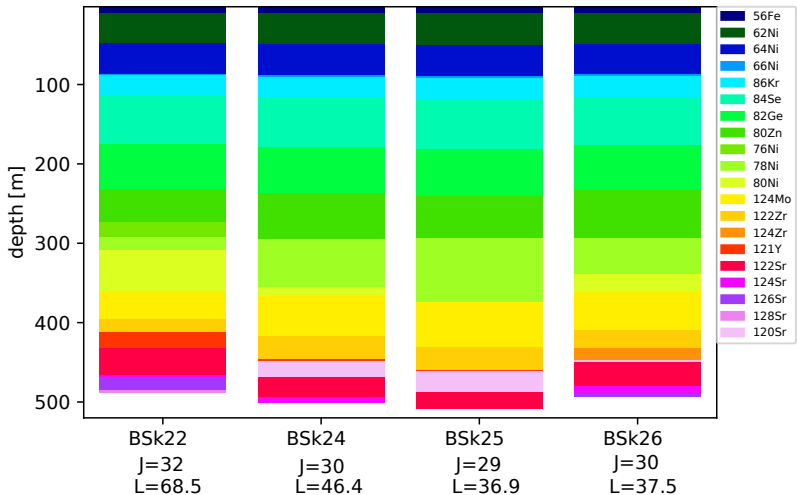
BSk vs chiral EFT

BSk22-26 are in fairly good agreement with recent calculations based on chiral effective-field theory at N3LO from Drischler et al. (2020):



BSk22-26 were NOT fitted to these chiral EFT calculations.

Role of the symmetry energy in the outer crust

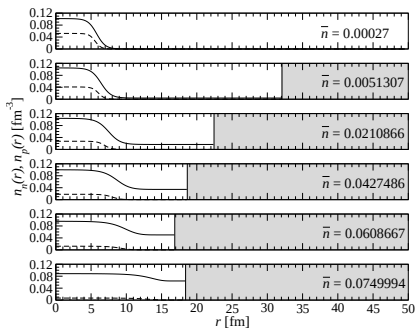
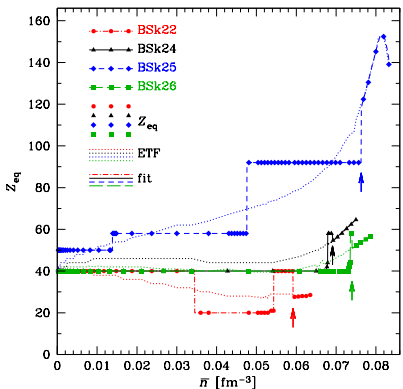


Structure of a neutron star of mass $1.5M_{\odot}$ and radius 13 km (figure prepared by A. F. Fantina)

Pearson et al., MNRAS 481, 2994 (2018)

Role of symmetry energy in the inner crust

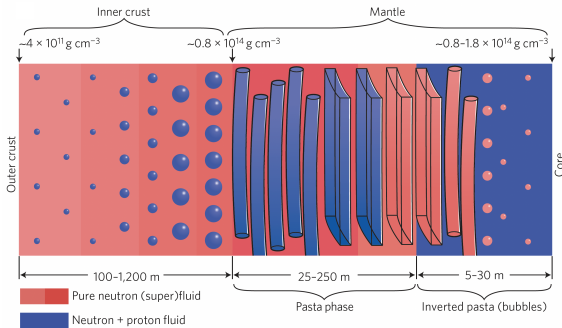
The composition of the inner crust is strongly influenced by the symmetry energy but also by proton shell effects:



Nuclear pastas in neutron stars

According to recent liquid-drop model calculations, pastas could represent about **50% of the mass of neutron-star crust**.

e.g. *Newton et al. EpJA58, 69 (2022); Dinh Thi et al., A&A 654, A114 (2021)*

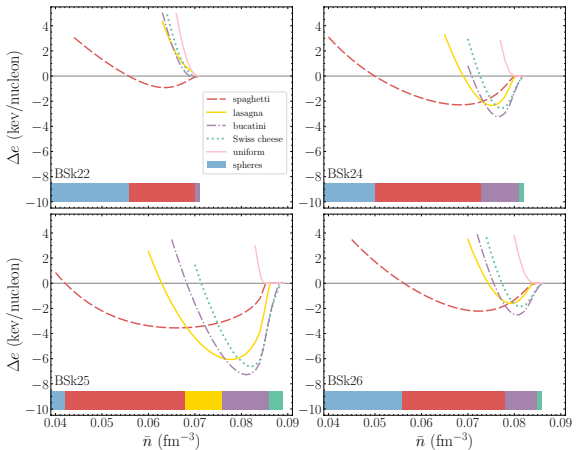


W. G. Newton, Nature Phys. 9, 396 (2013)

Pastas could have implications for thermal and dynamical evolutions of neutron stars and their magnetic field, gravitational-wave emission.

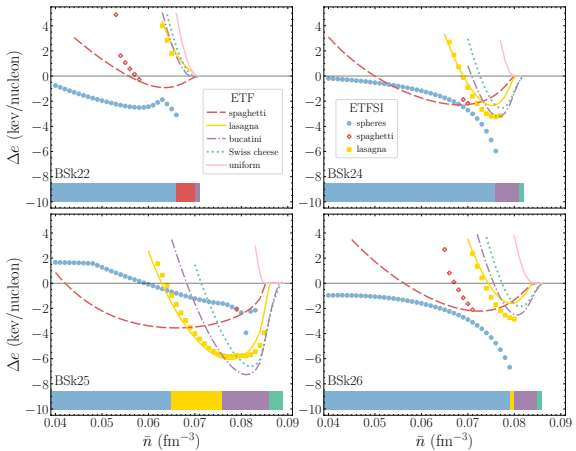
Nuclear pastas and symmetry energy - ETF

Pasta phases are more likely to appear for models with higher values of the symmetry energy at the relevant densities (BSk22 vs BSk25):



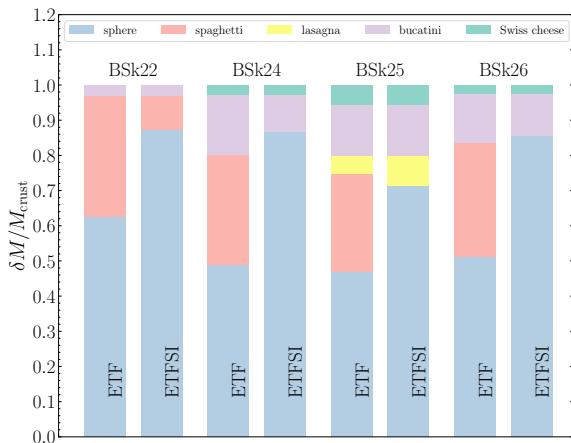
Nuclear pastas and symmetry energy - ETFSI

Pasta phases occupy a much narrower range of densities, and correlations with symmetry energy vanish:



Nuclear pastas abundances in neutron stars

The pasta mantle shrinks dramatically with shell effects!



Role of the nucleon density parametrization

At very high densities, results are sensitive to the choice of the parametrization of $n_q(\xi)$ in the Wigner-Seitz cell of “radius” R .

Writing the nucleon density as $n_q(\xi) = n_{Bq} + n_{\Lambda q} f_q(\xi)$,
the popular ansatz (n_{Bq} , $n_{\Lambda q}$, C_q , a_q are free parameters)

$$f_q^{\text{FD}}(\xi) = \frac{1}{1 + \exp\left(\frac{\xi - C_q}{a_q}\right)}$$

does not satisfy the boundary condition $\frac{dn_q}{d\xi}(\xi = R) = 0$.

Role of the nucleon density parametrization

At very high densities, results are sensitive to the choice of the parametrization of $n_q(\xi)$ in the Wigner-Seitz cell of “radius” R .

Writing the nucleon density as $n_q(\xi) = n_{Bq} + n_{\Lambda q} f_q(\xi)$,
the ansatz we adopted since 2008

$$f_q^{\text{StrD}}(\xi) = \frac{1}{1 + \exp \left[\left(\frac{C_q - R}{\xi - R} \right)^2 - 1 \right] \exp \left(\frac{\xi - C_q}{a_q} \right)}$$

does satisfy $\frac{dn_q}{d\xi}(\xi = R) = 0$ but all derivatives actually vanish.

Onsi et al., Phys.Rev.C77,065805 (2008)

Role of the nucleon density parametrization

At very high densities, results are sensitive to the choice of the parametrization of $n_q(\xi)$ in the Wigner-Seitz cell of “radius” R .

Writing the nucleon density as $n_q(\xi) = n_{Bq} + n_{\Lambda q} f_q(\xi)$,
our new ansatz is

$$f_q^{\text{SoftD}}(\xi) = \frac{1}{1 + \left(\frac{C_q - R}{C_q} \right)^2 \left(\frac{\xi}{\xi - R} \right)^2 \exp \left(\frac{\xi - C_q}{a_q} \right)}$$

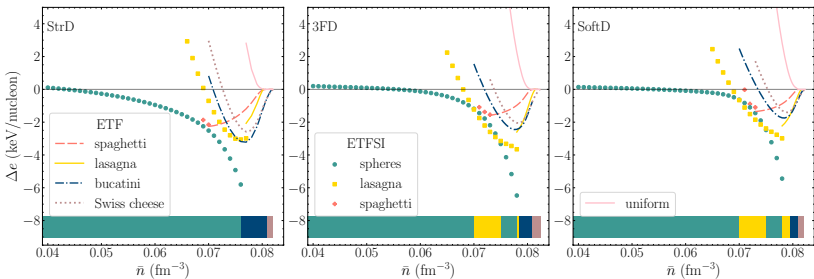
satisfies $\frac{dn_q}{d\xi}(\xi = 0) = \frac{dn_q}{d\xi}(\xi = R) = 0$.

We also consider

$$f_q^{3\text{FD}}(\xi) = f_q^{\text{FD}}(-\xi) + f_q^{\text{FD}}(\xi) + f_q^{\text{FD}}(2R - \xi) - f_q^{\text{FD}}(-R) - 2f_q^{\text{FD}}(R)$$

Role of the nucleon density parametrization

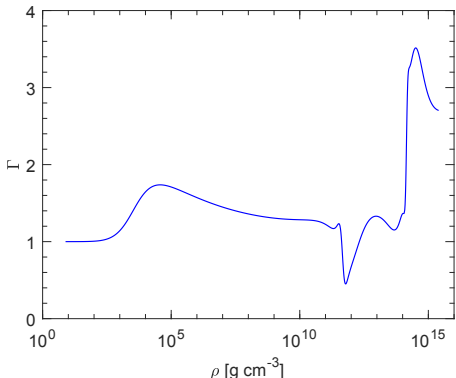
- All parametrizations agree up to the point where pastas first appear at $\bar{n} \approx 0.07 \text{ fm}^{-3}$.
- The two new parametrizations yield more stable configurations (lower energies).
- Both predict lasagna interspersed among gnocchis.



Unified equations of state

We have constructed **thermodynamically consistent** equations of state for all regions of a neutron star: outer and inner crusts, pasta mantle, and core using the **same nuclear functionals**.

Fantina et al., A&A 559, A128 (2013); Pearson et al., MNRAS 481, 2994 (2018)



Unified equations of state can hardly be parametrized by polytropes!

$$\Gamma \equiv \left(1 + \frac{P}{\rho c^2} \right) \frac{d \log P}{d \log \rho}$$

Direct Urca cooling vs observations

EoS	n (fm $^{-3}$)	ρ (g cm $^{-3}$)	M_{DU}/M_{\odot}
BSk22	0.33	5.88×10^{14}	1.15
BSk21/24	0.45	8.25×10^{14}	1.60
BSk25	0.47	8.56×10^{14}	1.61
BSk19/20/26	—	—	—

The very fast direct Urca cooling process is required to explain

- the thermal luminosities of some accreting neutron stars in quiescence (e.g. SAX J1808.4–3658)
- the thermal relaxation of some transiently accreting neutron stars (e.g. MXB 1659–29).
- the cooling of cold young isolated neutron stars.

Marino et al., Nature Astron. 8, 1020 (2024)

- The dUrca process is allowed in all models but BSk19/20/26.
- The low value for M_{DU} predicted by BSk22 implies that dUrca would operate in most neutron stars at variance with observations, but could be suppressed by superfluidity.

NICER and XMM Newton observations

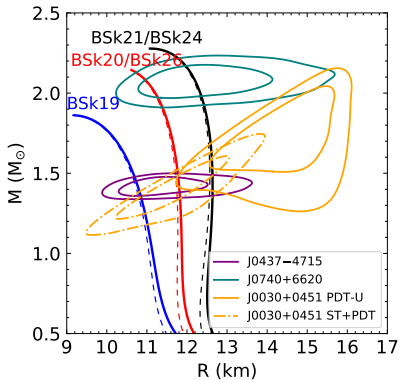


Figure from Lami Suleiman
Fantina et al., A&A 665, A74 (2022)

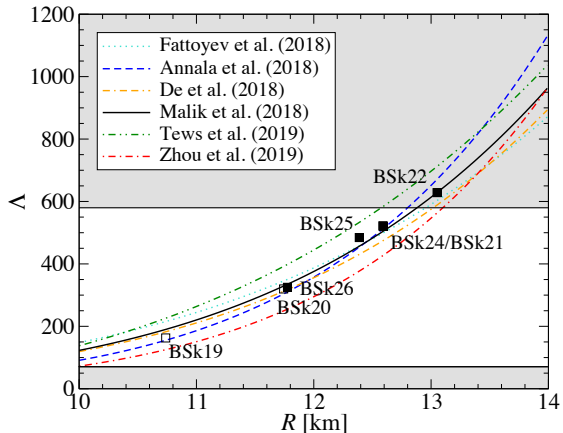
Analyses of NICER and XMM Newton observations:

- PSR J0030+0451
Vinciguerra et al., ApJ, 961, 62 (2024)
- PSR J0437-4715
Choudhouri et al., ApJL 971, L20 (2024)
- PSR J0740+6620
Riley et al., ApJL 918, L27 (2021)

- BSk19 is too soft to explain PSR J0740+6620.
- BSk20/26 could be marginally consistent with PSR J0030+0451.

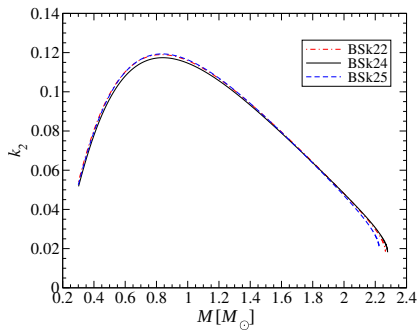
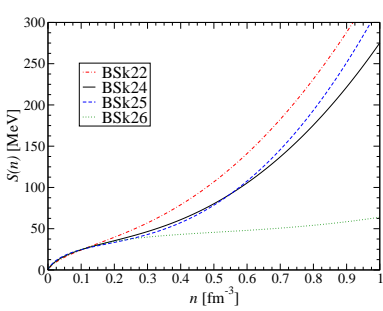
Tidal deformability of neutron stars

The tidal deformability coefficient Λ of a $1.4M_{\odot}$ neutron star is strongly correlated with R hence also with the symmetry energy:



Symmetry energy and Love number

The Love number k_2 is insensitive to the symmetry energy:

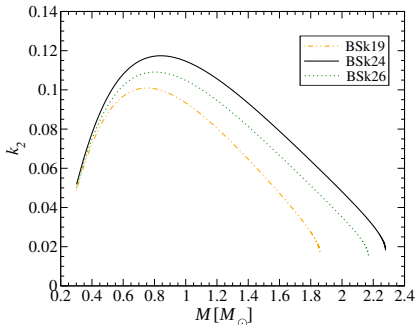
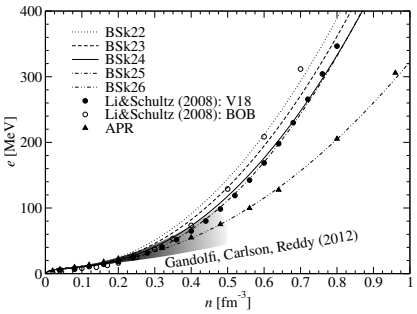


Perot, Chamel, Sourie, Phys. Rev. C 100, 035801 (2019)

The dependence of $\Lambda = (2/3)k_2(Rc^2/GM)^5$ on the symmetry energy thus arises mainly from the factor R^5 .

Neutron matter and Love number

The Love number is mostly governed by the neutron-matter stiffness: the softer the equation of state, the lower k_2 is.



Perot, Chamel, Sourie, Phys. Rev. C 100, 035801 (2019)

Same kind of correlations for higher-order tidal coefficients.

Perot & Chamel, Phys. Rev. C 103, 025801 (2021)

Role of the “crust” on the tidal deformability

Different approaches with different conclusions:

Piekarewicz & Fattoyev

Phys. Rev. C99, 045802 (2019)

- BPS for the outer crust (using Duflo & Zuker mass table)
- RMF (FSUGarnet) for the core
- polytropes for the inner crust

$\delta\Lambda_{1.4}/\Lambda_{1.4} \lesssim 0.1\%$ when varying the polytropic index

Ji et al., Phys. Rev. C100, 045801(2019)

Kalaitzis, Motta, Thomas

Int. J. Mod. Phys. E28, 1950081 (2019)

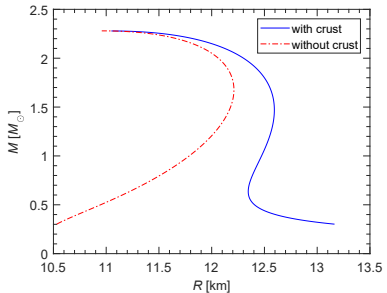
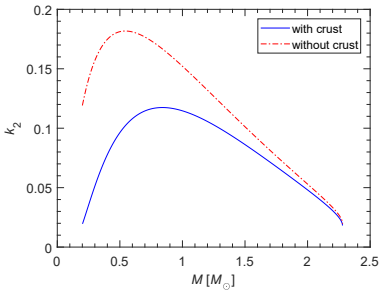
tabulated EoSs fitted using two polytropes for the core

$\delta\Lambda_{1.4}/\Lambda_{1.4} \lesssim 10\%$ when comparing to fitted EoS extrapolated to lower densities

$\delta\Lambda_{1.4}/\Lambda_{1.4} \sim 3\%$ when matching different crusts to the same core

Role of the crust on the tidal deformability

Comparison with purely homogeneous neutron stars for BSk24:



Perot et al., Phys. Rev. C 101, 015806 (2020)

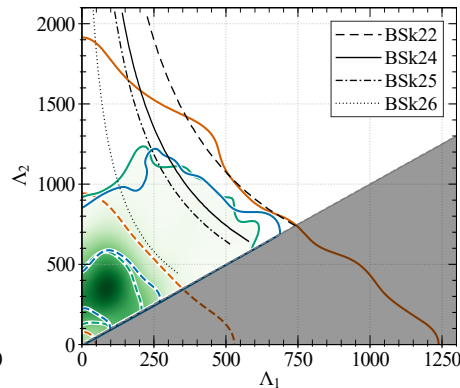
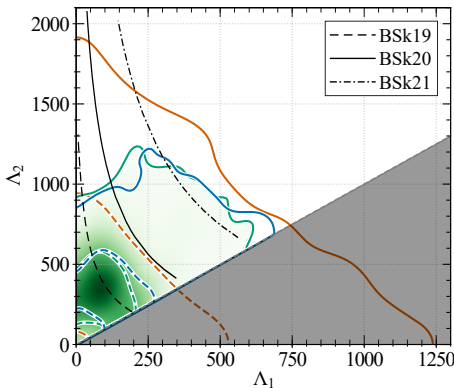
- Changes in k_2 are essentially due to ΔR (analytic formula)
- Changes in $\Lambda \propto k_2 R^5$ are small ($< 1\%$): the strong reduction of k_2 is compensated by the increase of R
- Elastic effects are completely negligible

The crust may still lead to $\sim 1\%$ systematic errors on the radii inferred from the analysis of the gravitational-wave signal

Gamba et al., Class. Quantum Grav. 37, 025008 (2020)

LIGO-Virgo observations of GW170817

The detection of GW170817 by the LIGO-Virgo collaboration provided the first measurement of the tidal deformability of neutron stars:



Perot, Chamel, Sourie, Phys. Rev. C 100, 035801 (2019)

A stiff symmetry energy (BSk22) is marginally compatible.

Conclusions

We have constructed **thermodynamically consistent** equations of state for neutron stars based on accurately calibrated functionals varying the neutron-matter stiffness and symmetry energy:

Pearson et al., MNRAS 481, 2994 (2018)

Tables available on CompOSE: <https://compose.obspm.fr/>
PCP(BSk22), PCP(BSk24), PCP(BSk25), PCP(BSk26)

Freely available computer code for the outer crust:

<http://doi.org/10.5281/zenodo.3719439>

Gravito-electric and magnetic Love numbers up to $\ell = 5$:

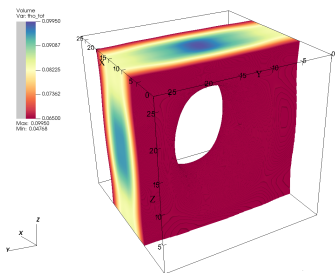
Perot&Chamel, Phys. Rev. C 103, 025801 (2021)

Our currently preferred model consistent with chiral EFT calculations and astrophysical observations is **BSk24**.

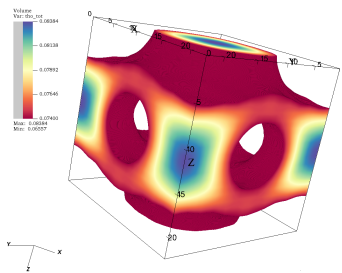
Perspectives

- **Extension to finite temperatures** for neutron-star mergers
(Chiranjib Mondal)
- **New functionals at N2LO** (Guilherme Grams, Wouter Ryssens)
- **Full 3D HFB calculations** of nuclear pastas (Nikolai Shcheculin)

DB: den_pl_nb=0.065_Z=46.0_A=1444_L=14.1_full_box.wtxt



DB: den_cyl_nb=0.074_Z=30.0_A=950_L=11.7_full_box.wtxt



- **Full 3D TDHFB simulations** of neutron superfluidity in the crust
(Piotr Magierski, Gabriel Włazłowski, Daniel Pęcak)